LAWRENCE
LIVERMORE
NATIONAL
LABORATORY

LLNL-JRNL-546911

3D Effects in Geomagnetic EMP Computations

H. W. Kruger

April 11, 2012

Journal of Radiation Effects Research and Engineering

Disclaimer

This document was prepared as an account of work sponsored by an agency of the United States government. Neither the United States government nor Lawrence Livermore National Security, LLC, nor any of their employees makes any warranty, expressed or implied, or assumes any legal liability or responsibility for the accuracy, completeness, or usefulness of any information, apparatus, product, or process disclosed, or represents that its use would not infringe privately owned rights. Reference herein to any specific commercial product, process, or service by trade name, trademark, manufacturer, or otherwise does not necessarily constitute or imply its endorsement, recommendation, or favoring by the United States government or Lawrence Livermore National Security, LLC. The views and opinions of authors expressed herein do not necessarily state or reflect those of the United States government or Lawrence Livermore National Security, LLC, and shall not be used for advertising or product endorsement purposes.

3D Effects in Geomagnetic EMP Computations

Hans Kruger
Lawrence Livermore National Laboratory

Abstract

The MCNP coupled gamma/electron Monte Carlo transport code, developed by the Los Alamos National Laboratory, and the author's MACSYNC 3D Monte Carlo synchrotron-radiation-based geomagnetic EMP code have been used to investigate the impact of 3D effects that cannot be treated by such widely used legacy 1D spherically symmetric geomagnetic EMP codes as CHAP. Several effects were found to significantly alter the computed EMP. In particular, electron multiple scattering effects on the instantaneous position of the radiating electrons place a lower bound on the rise time which is an order-of-magnitude longer than rise times computed by CHAP and used to formulate current EMP hardening standards.

Introduction

The CHAP geomagnetic EMP code has been used at Lawrence Livermore National Laboratory (LLNL) since the 1980's to compute EMP generated by LLNL's nuclear warhead designs.[1] CHAP is a one-dimensional spherically symmetric code and it uses certain simplifying physics approximations to be discussed in this paper. For the past few years, the author has been investigating the potential effects of these CHAP limitations on computed EMP rise times and shapes. This is a progress report on that effort.

Three effects that can spread the position of the radiating Compton electrons along the line-of-sight (LOS) from the burst point to the observer, and thereby spread the pulse rise time, were investigated. These are electron multiple scattering, angular distribution of Compton electron generation, and bending of the electrons by the magnetic field. Two effects that can impact the general shape of the pulse were also examined. One effect is due to differences in EM attenuation by air conductivity between EMP emitted by electrons created on the LOS and those created off the LOS. This attenuation difference is due to differences in conduction electron attachment during the interval between air conductivity creation and EMP arrival. The other effect investigated is time and place of Compton electron creation by multiply scattered gammas and their interaction with the on-off-LOS attenuation effect.

For this investigation, the author used the well-known MCNP coupled photon-electron Monte Carlo transport code, developed by Los Alamos National Laboratory (LANL), and his own 3D MACSYNC geomagnetic EMP code.[2]

MCSYNC Geomagnetic EMP Code

MCSYNC is fully three-dimensional. It uses MCNP as a subroutine to transport gammas and electrons. There are typically a few thousand electron transport steps. At the end of each transport step, MCSYNC uses the instantaneous position and velocity vector of the electron to generate a synchrotron radiation mini-pulse in the direction of the observer. The shape of the synchrotron radiation beacon as a function of electron energy is shown in Fig. 1. This figure displays the component of the electric field in the plane of the electron orbit. It is given by the equation

$$zE_x = (8.45e\text{-}11)B\beta(1-\beta^2)^{0.5}(\beta U^2-(1-\beta W)W)/(1-\beta W)^3,$$

where zE_x is the product of electric field in the orbit plane and distance along the z-axis in units of Volt per Compton electron, B is the magnetic field in the y direction in gauss, β is the electron velocity in units of the speed of light, and U and W are the direction cosines with the x- and z-axis, respectively.

This equation is derived from an equivalent equation given by Sokolov and Ternov by expressing it in the coordinate system used in MCSYNC.[3] Here the source is at the origin of a Cartesian coordinate system, the observer is located on the z-axis, while the magnetic field is directed along the y-axis. There is also an electric field perpendicular to the electron orbit. For a Compton electron distribution that is symmetric about the LOS, which is the case for this investigation, the net perpendicular field is null.

At the end of each electron transport step, the synchrotron radiation mini-pulse is propagated from the instantaneous position of the electron to the observer. The pulse is attenuated along that path by the intervening air conductivity. At the observer, the mini-pulses are tallied into observer-time-of-arrival bins and added in each time bin, resulting in a composite electromagnetic pulse.

MCSYNC uses two different models for the attenuation depending on burst altitude. For near-surface bursts, where the high air density results in a relatively short conduction electron attachment time constant, the code uses a radius and time dependent conductivity model derived from fits to high-spatial-resolution, time-dependent MCNP calculations modified for time-dependent conduction electron attachment. These calculations were done for specific gamma energies or gamma spectra of interest. An example of the conductivity model is shown in Fig. 2 for 3 Mev gammas in sea level air for a 0.1 shake wide step gamma output pulse and a one shake conduction electron attachment time constant (1 shake equals 10 nanoseconds). In this Figure, the contribution to total conductivity from unscattered gammas, scattered gammas, and ions are shown separately at different ranges from the burst point.

For high-altitude bursts, a simpler approach has been used, since conduction electron attachment can be ignored because the attachment time constant rapidly increases with

altitude, being roughly inversely proportional to air density squared. The EMP attenuation is computed separate from the MCSYNC calculation using the author's EMATT code and then applied to the MCSYNC results. EMATT calculates attenuation vs. altitude along a given LOS in a spherical earth geometry using an analytic air conductivity model based on gammas depositing all their energy at the first Compton scatter event.

MACSYNC is a very efficient three-dimensional EMP code since CPU time is only linearly dependent on the desired time resolution, which is determined by the electron transport step size. In conventional methods of solving Maxwell's equations on a 3D grid, the required CPU time is very much longer since it is proportional to the fourth power of the time resolution. A disadvantage of MACSYNC is that the field is not known until the end of the calculation. As a consequence, the effect of the electric field on the electron's motion is not treated. In principle, this could be done by iterating the calculation, however, this is awkward. Fortunately, this effect does not matter for the current calculations, which deal principally with EMP generation at lower altitudes. The range of the electrons at these altitudes is sufficiently short that typical EMP fields cannot change the electron's energy significantly.

Effects on Rise Time

Multiple Electron Scattering and Compton Electron Emission Angles

As Compton electrons move through the air, they experience multiple successive scattering through Coulomb interactions with air molecules. Electrons, starting out as a delta function pulse heading towards the observer, will spread out in space. In particular, they will be spread out in distance along the LOS to the observer, which determines the arrival time of EMP at a distant observer. This is shown in the results of MCNP calculations, displayed in Fig. 3, for a delta function pulse of 1 or 3 Mev electrons emitted from a point source at an altitude of 34 km with an air density of 1e-5 g/cc. The electrons are emitted either as a pencil source along the LOS or as cone source distributed uniformly in angle between the LOS and either 30 or 15 degrees with the LOS. These two angles are the average Compton electron emission angle for 1 and 3 Mev gammas, respectively. The purpose of using these emission angles is to assess the effects of the Compton electron angular distribution on spatial spreading.

Fig. 3 shows snapshots of the electron distribution along the LOS at different times in the electrons' history corresponding to an average energy loss of 10, 20, 50, or 80 percent. As soon as the electrons are born, they feel the magnetic field and they begin to radiate. That radiation continues until the electrons come to rest. It can be seen in the Figure that the electrons fall farther behind the first emitted EMP and spread out as they continue to lose energy and undergo multiple scattering. The space between the first emitted EMP and the instantaneous electron position along the LOS is filled with EMP. As an example, as can be seen from this Figure, when 1 Mev electrons have lost 50% of their energy, they have spread out over almost 200 m along the LOS. On the average, the electrons are now about 80 m behind the first emitted EMP. This results in an EMP arrival

time spread at the observer of about 240 nanoseconds. The emission of the Compton electrons at an angle with the LOS increases the spatial spread and the associated EMP arrival time spread.

Bending by the magnetic field will also contribute to spreading out of the electrons along the LOS. Fig. 4 displays MCNP calculations for 1 Mev electrons similar to those shown in Fig. 3, comparing spreading with and without a magnetic field of 0.3 gauss. The calculations are for an altitude of 34 km (1e-5g/cc air density) or 18 km (1e-4 g/cc air density). It can be seen that the magnetic field significantly increases the spreading at the higher altitude, but that there is a negligible effect at the lower altitude. The reason for this is that the electron range at the lower altitude is an order-of-magnitude shorter and not large enough for the electrons to experience much bending. Because this paper is mainly concerned with finding a lower bound on the EMP rise time and since the shortest rise times occur at low EMP generation altitudes, magnetic field effects on electron spreading have been neglected.

An EMP arrival time spread will result in a similar EMP rise time. For this reason, proper treatment of the effect of electron multiple scattering on the position of the radiating electron is important if an EMP code is to produce a correct pulse rise time. CHAP treats multiple scattering approximately through the use of a so-called obliquity factor which is based on the root-mean-square scattering angle. CHAP solves the equations of motion for the electron using the unscattered velocity.[4] It then corrects the resulting current magnitude for the fact that multiple scattering has reduced the electron velocity along the LOS, using the obliquity factor. However, CHAP does not correct the position of the radiating electron for this effect; its position relative to the first emitted EMP is solely determined by its velocity adjusted only for average energy loss. This physics approximation turns out to significantly decrease the EMP rise time computed by CHAP.

The EMP arrival time spread at the observer with and without adjusting the radiating electron position for multiple scattering is shown in Fig. 4. These spread sheet calculations use tabulated stopping power values for the arrival time spread without treatment of multiple scattering, and a root-mean-scattering angle when multiple scattering is treated.[5,6] The arrival time spread is shown as a function of electron energy for either an average energy loss of 20% or 50%. It can be seen that neglecting the effect of multiple scattering on the instantaneous position of the radiating electron underestimates the EMP arrival time spread by an order of magnitude for all electron energies. Further, calculations without treatment of the effect of multiple scattering on electron position incorrectly suggest that increasing the Compton electron energy, by increasing the gamma energy, will produce very small arrival time spreads and associated short EMP rise times.

The connection between EMP arrival time spread and pulse rise time is illustrated in Fig. 5. The MACSYNC calculation shown in this Figure used a 100 km radius electron source surface centered on the z-axis, which points at the distant observer. The electron pulse width is 0.01 sh, the electron energy is 3 Mev, the air density is 1.2e-5 g/cc corresponding to an altitude of 33 km, and there is no EM attenuation between the radiating electrons

and the observer. The electrons are either emitted along the surface normal or uniformly in an angular interval between the surface normal and an angle of 15 degrees with the surface normal. Again, the purpose of latter case is to test for the effect of the angular distribution of Compton electron emission by gammas.

Two sets of normalized rE are shown in Fig. 5, where r is the distance to the observer and E is the radiated electric field. One set is for an electron point source located on the z-axis, while the other set is for sources distributed uniformly over the spherical surface. For the point source, the electric field drops rapidly with a tail extending well beyond 20 sh of observer time. The field drops because it is a steep function of the electron energy, with a 20% energy loss reducing the field by a factor of two and a 50% energy loss reducing it by a factor of ten. For the surface source, the field is the composite of the fields from all point sources on the surface. The field from points on the z-axis arrives first, followed by fields from off-axis points, which arrive later because these source points are farther away from the observer. It can be seen that the composite field rises for a duration equal to the base width of the point source field. It can also be seen that the emission of the electrons with an angle to the surface normal increases the width of the point source field. This is expected because such off-normal emission angles will lead to a greater spreading of the electrons along the LOS as shown in Fig. 3. The wider point source field, in turn, produces a wider rise time of the composite field.

Figs. 7 – 10 show results of MACSYNC calculations for an isotropic gamma point source at an altitude of 100 km in an exponential atmosphere directly above a ground-based observer. In these calculations, the gammas generate Compton electrons with their full angular and correlated energy distribution. The gamma energy is parametrically varied between 1 and 9 Mev. The atmosphere is modeled with a stack of 2 km high planar zones between the burst point and the ground with each zone having an average air density corresponding to its average altitude. The energy of the gammas is 1, 3, 6, and 9 Mev in Figs. 7 – 10, respectively. These Figures show the rise time part of the composite EMP pulse at the observer separately for EMP generated in each of the air layers, starting with the layer at 33 km altitude (air density 1.1e-5 g/cc) and ending with the layer at 17 km altitude (air density 1.1e-4 g/cc). Inspection of Figs. 7 – 10 shows that the EMP amplitude decreases with decreasing generation altitude. Between 33 and 17 km altitude, this decrease ranges from more than two orders-of-magnitude at 1 Mev to one order-of-magnitude at 9 Mev.

The lower-altitude layers plotted in Figs. 7 - 10 were chosen because the focus of this paper was on establishing a lower bound on the EMP rise time. As can be seen from these Figures, the rise time due to multiple scattering decreases as the air density at the location of the electrons increases. This is consistent with the first-principles expectation that the arrival time spread should be inversely proportional to the density of the air in which the electrons are moving. This expectation is based on the fact that density sets the electron’s range and the distance it falls behind along the LOS for a given root-mean-square (rms) scattering angle. This rms angle depends only on the total mass per unit area traversed and is thus the same for a given electron fractional energy loss

independent of local air density. Note that the MCNP calculations shown in Fig. 4 for 1e-5 and 1e-4 g/cc density air show the expected dependency on air density.

Thus, to produce the shortest possible EMP rise time from a high-altitude burst, it is necessary to produce Compton electrons at the lowest possible altitude and prevent EMP generated by Compton electrons at higher altitudes from reaching the ground observer. As can be seen from the EMATT computations plotted in Fig. 11, the former requires placing the burst over the ground observer and maximizing the gamma energy, while the latter is accomplished by increasing the gamma yield which, in turn, increases the air conductivity and associated EM attenuation at higher altitudes sufficiently to black-out EMP generated at the higher altitudes.

Lower Bound on EMP Rise Time

Computations presented above show that the EMP rise time is dominated by electron multiple scattering effects and that these effects cause a rise time that is inversely proportional to the air density at the altitude at which the radiation is generated. A round number of 15 shakes or 150 nanoseconds appears to be a reasonable estimate for a lower bound on rise time for a delta function gamma output pulse and a radiation generation altitude of 30 km. Starting with this number, the lower rise time bound for lower altitudes can be obtained by scaling inversely with air density. The result is shown in Fig. 12.

There are two scenarios for which EMP rise time is of particular interest. One scenario is observation from space of nuclear detonations on the ground or at some other altitude at which detectable EMP is produced. Here a short rise time is important because it determines the penetration of the ionosphere. The other scenario is a high-altitude detonation observed on the ground. The first scenario deals with such issues as treaty verification or tactical warning. The second scenario relates to such matters as EMP hardening standards or military applications of EMP.

Fig. 12 shows the range of lower rise time bounds for these two scenarios. For detonations within the atmosphere observed from space, the radiation generation altitude is approximately given by the detonation altitude. Thus the lower rise time bound, for a delta function gamma output, is approximately 2 nanoseconds for ground bursts, extending to approximately 150 nanoseconds for 30 km bursts.

For high-altitude detonations observed on the ground, the dominant radiation altitude depends on the gamma yield and the ground distance between the detonation sub-point and the observer, as can be seen in Fig. 11. In particular, for ground ranges intermediate between the sub-point and the burst horizon, the dominant radiation altitude will be roughly 30 km for low yields, while for high yields it will be roughly 20 km. Thus for this geometry the lower rise time bound, for a delta function gamma output, is approximately 150 nanoseconds for low-yield and approximately 30 nanoseconds for high-yield bursts.

For purposes of setting pulse rise times for EMP hardening standards, the challenge is choosing the shortest achievable pulse rise time. The results presented in this paper suggest that a good estimate for this rise time is of the order of tens of nanoseconds. This estimate is an order-of-magnitude longer than the few-nanosecond rise time of the pulse used for the unclassified EMP hardening standard MIL-STD-464 (Fig.13).[7] This hardening standard was based on EMP computations performed by the nuclear design laboratories and DTRA contractors using CHAP and other similar legacy one-dimensional spherical codes. It appears that the short rise time of MIL-STD-464 is an unphysical artifact caused by electron multiple scattering physics simplifications in these codes. Compton electrons can generate nanosecond EMP rise times only when they are created in sea level density air, however, weapon output gammas cannot penetrate the atmosphere to sea level from a high-altitude burst.

Effects on Pulse Shape

For bursts at very low altitudes, the attachment time for conduction electrons is sufficiently short as to allow removal of conduction electrons between the time of their creation by the Compton electrons at some region on the propagation path to the observer, and the time when the EMP traverses this region. This is illustrated in Fig. 14 for a 1 kT ground burst. For EMP generated on the direct burst-to-observer LOS, there is very little delay between conduction electron creation and EMP arrival, compared to the attachment time constant in sea level air of approximately 1 shake. Thus there is negligible reduction of conduction electron density along this propagation path. However, for EMP that is generated off the direct LOS, the delay can be large compared to the 1 shake attachment time constant.

For a 1 kT burst in sea level air, the air conductivity will completely absorb all EMP generated within ~1 km radius. The region between 1 and 2 km is semitransparent, and that beyond 2 km is completely transparent to EMP. When the spherical divergence and exponential attenuation of the gammas are considered, most of the EMP reaching a distant observer is found to have been generated in the semitransparent shell. For this reason, three relevant parameters are plotted in Fig. 14 for EMP generated at a 1 km radius at an off-LOS angle theta and subsequently attenuated by a conduction electron density n_e located on the propagation path at a 1.5 km radius. These parameters are the time available for attachment, the factor by which n_e is reduced during this time, based on a 1 shake sea level attachment time constant, and the arrival time difference at the observer between the EMP generated on-LOS and off-LOS. For a delta function gamma output, this on-off-LOS time difference corresponds to the time within the electromagnetic pulse measured from the leading edge of the pulse. For example, as can be seen from Fig. 14, 10 shakes or 100 nanoseconds after the leading edge of the EMP, at an angle theta of ~28 degrees, the time available for attachment is ~33 nanoseconds or ~3.3 shakes, resulting in a reduction of n_e by a factor of e+3.3=27.

MACSYNC calculations, showing the effect of this on-off-LOS difference in EMP attenuation in detail, are displayed in Fig. 15. The calculations used a near-surface burst

with a total yield of 1 kT with a 0.01 shake step output pulse of 3 Mev gammas with a gamma yield of 0.3%. The two lower curves show calculations in which the gammas were stopped after their first Compton scatter event. The two upper curves show calculations in which the gammas were allowed to multiply scatter until their energy dropped below a small fraction of an Mev. For both pairs of curves, the upper curve of each pair shows calculations that included the on-off-LOS attenuation difference. The lower curve of each pair does not allow such a difference.

It can be seen from these curves that inclusion of the 3D effects, that produce on-off-LOS attenuation differences, matter. Even more important is inclusion of detailed time–dependent, fully 3D gamma transport that lets the multiply scattered gammas generate Compton electrons and the associated EMP at the proper place and at the proper time, so that the EMP will traverse the ionized air on its path to the observer at the proper time. Only under those conditions will there be a correct timing for off-LOS attenuation reduction. CHAP makes an approximate adjustment for multiply scattered gammas by multiplying the prompt gammas by a time-dependent build-up factor. This approach is incapable of placing these gammas at the correct position, resulting in incorrect timing of the associated EMP. HEMP-B, another 1D spherical legacy code similar to CHAP, does not treat multiply scattered gammas at all.[8] Neither CHAP nor HEMP-B, being one-dimensional spherical, are capable of treating on-off-LOS effects at all.

Conclusions and Observations

The 3D computations discussed in this paper lead the author to the following conclusions:

1. 3D effects significantly impact the computed EMP rise time and shape.
2. Electron multiple scattering imposes a lower bound on EMP rise time, which is an order-of-magnitude longer than the nanoseconds rise time of the pulse used in the unclassified EMP hardening standard MIL-STD-464. This hardening standard is based on legacy 1D spherically symmetric EMP code calculations. The short EMP rise time computed by these codes is an unphysical artifact caused by electron multiple scattering physics simplifications.

The author would like to offer these observations:

1. The 40-some year old legacy 1D geomagnetic EMP codes ought to be replaced with modern 3D codes. A code solving Maxwell's equations self-consistently on a 3D grid with detailed coupled gamma-electron Monte Carlo transport will provide excellent physics modeling, however, running such a code with the required time resolution will require very long clock times even on current super computers. For this reason, it would make sense to also patch a legacy code such as CHAP so that it could approximately treat the effect of multiple scattering on rise time. A patched CHAP could be used for fast engineering level computations of high-altitude bursts. However, it would not be useful for low-altitude bursts because it lacks the 3D capability needed to treat on-off-LOS effects and multiple scattering of gammas correctly.

2. The impact of 3D effects on EMP hardening standards, military applications of EMP, and space observation of EMP ought to be evaluated.

Acknowledgement

The author thanks Dr. Dennis Hewett for his encouragement and support, and Robert Palasek for assistance with programming and compilation issues.

Prepared by LLNL under Contract DE-AC52-07NA27344

References

1. H. J. Longley and C. L. Longmire, “Development of the CHAP EMP Code”, Mission Research Corporation Report DNA 3150T (1973).

2. Los Alamos National Laboratory X-5 Monte Carlo Team, “MCNP – A General Monte Carlo N-Particle Transport Code, Version 5”, LA-UR-03-1987 (2005).

3. A. A. Sokolov and I. M. Ternov, “Synchrotron Radiation”, Akademie–Verlag Berlin, Permagon Press, p.38 (1968).

4. C. L. Longmire, “The Early-Time EMP from High-Altitude Nuclear Explosions”, Mission Research Corporation Report MRC-R-809, p. 44 (1983).

5. M. J. Berger and S. M. Seltzer, “Tables of Energy Losses and Ranges of Electrons and Positrons”, National Bureau of Standards Report NASA SP-3012 (1964).

6. J. J. Hernandez et al, “Review of Particle Properties”, Physics Letters B (Elsevier Science Publishers), p. III-14 (1990).

7. Department of Defense Interface Standard, Electromagnetic Environmental Effects Requirements for Systems MIL-STD-464, 18 March 1997.

8. W. E. Page et al, “A Description of the HEMP-B Computer Code”, Air Force Weapons Laboratory Report AFWL-TR-73-286 (1975).

Figures

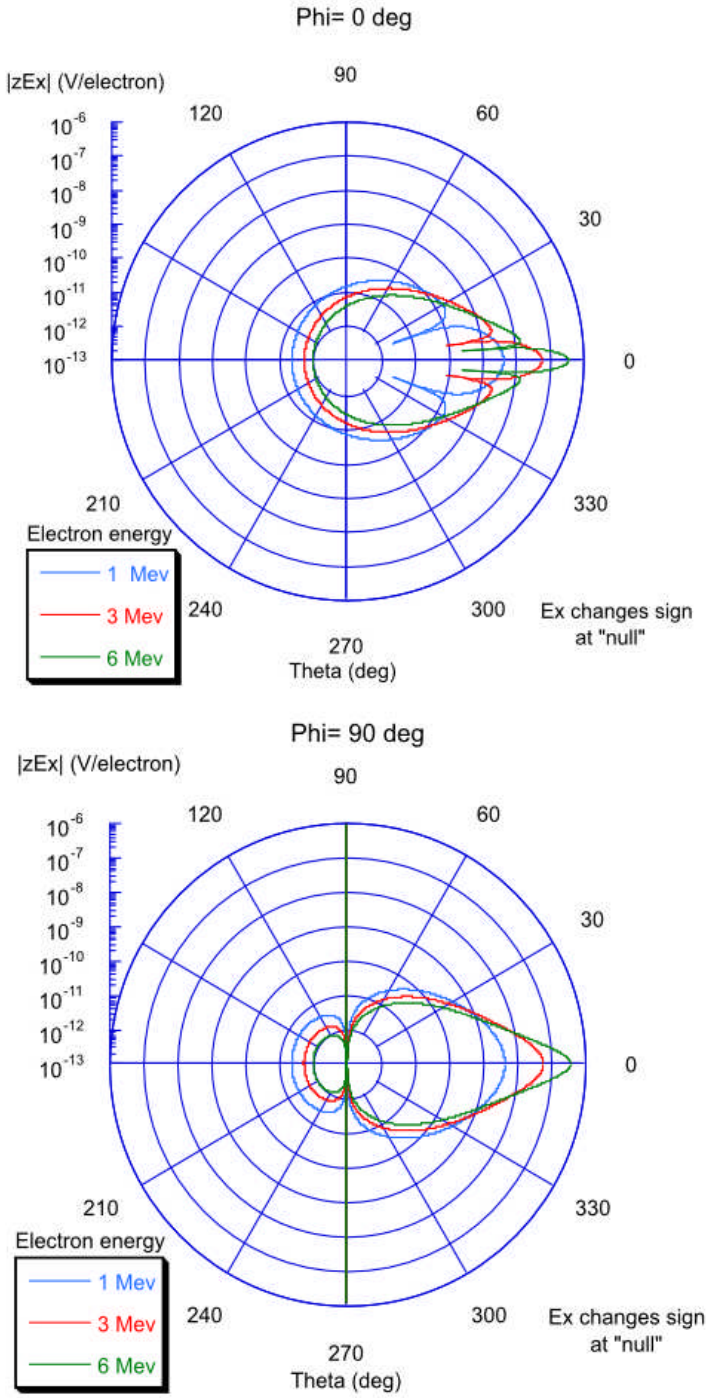

Fig. 1. The synchrotron radiation beam is not axially symmetric about the velocity vector and a steep function of the electron energy. Note that the field changes sign at the null.

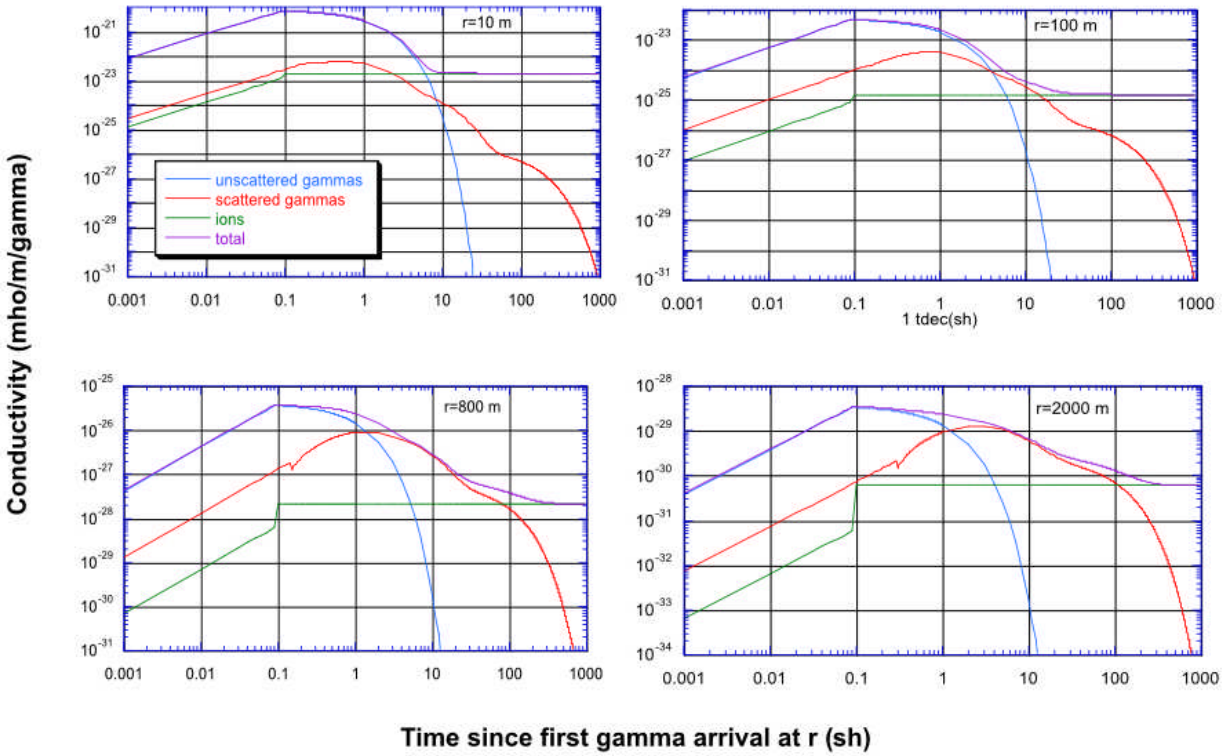

Fig. 2. Conductivities are based on time dependent energy deposition from 3D coupled gamma-electron high spatial resolution MCNP calculations adjusted for conduction electron attachment. Sea level air; 0.1 sh output step pulse of 3 Mev gammas; 1 sh attachment time.

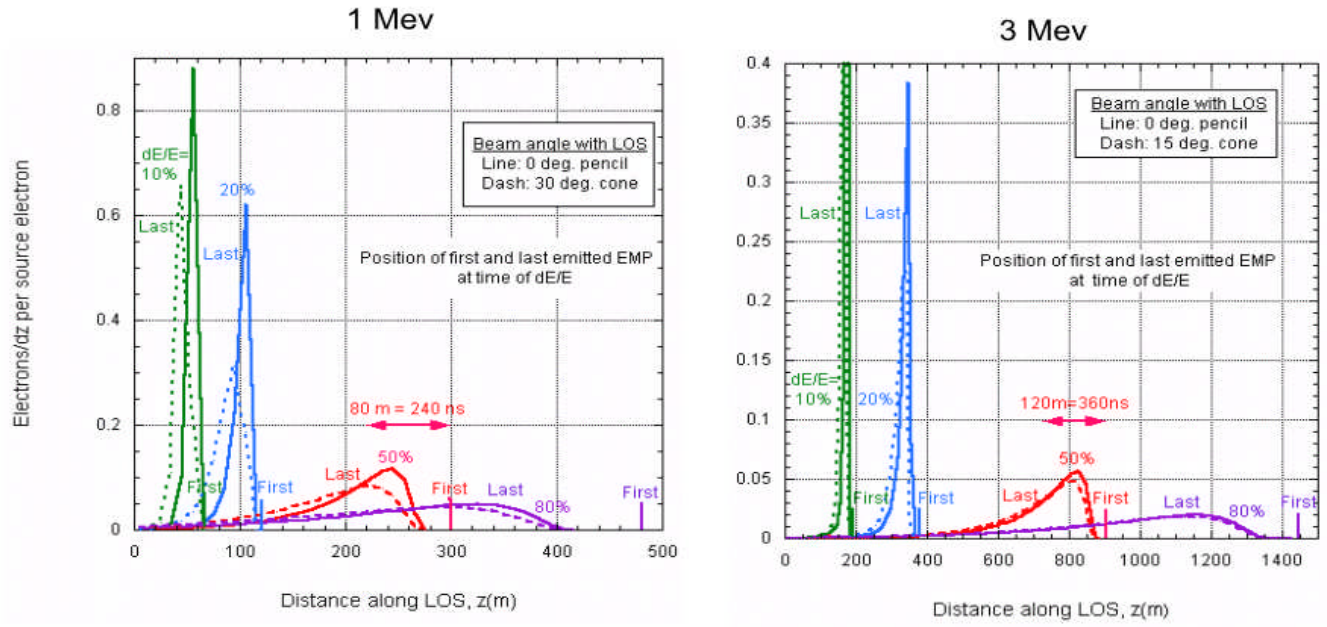

Fig. 3. These MCNP calculations show significant electron position spreading along the LOS between the burst and the observer due to electron multiple scattering. The source is an electron pencil beam directed either along the LOS at the observer or uniformly distributed in angle between the LOS and an angle of 15 degrees with the LOS. The air density is 1e-5 g/cc corresponding to an altitude of 34 km.

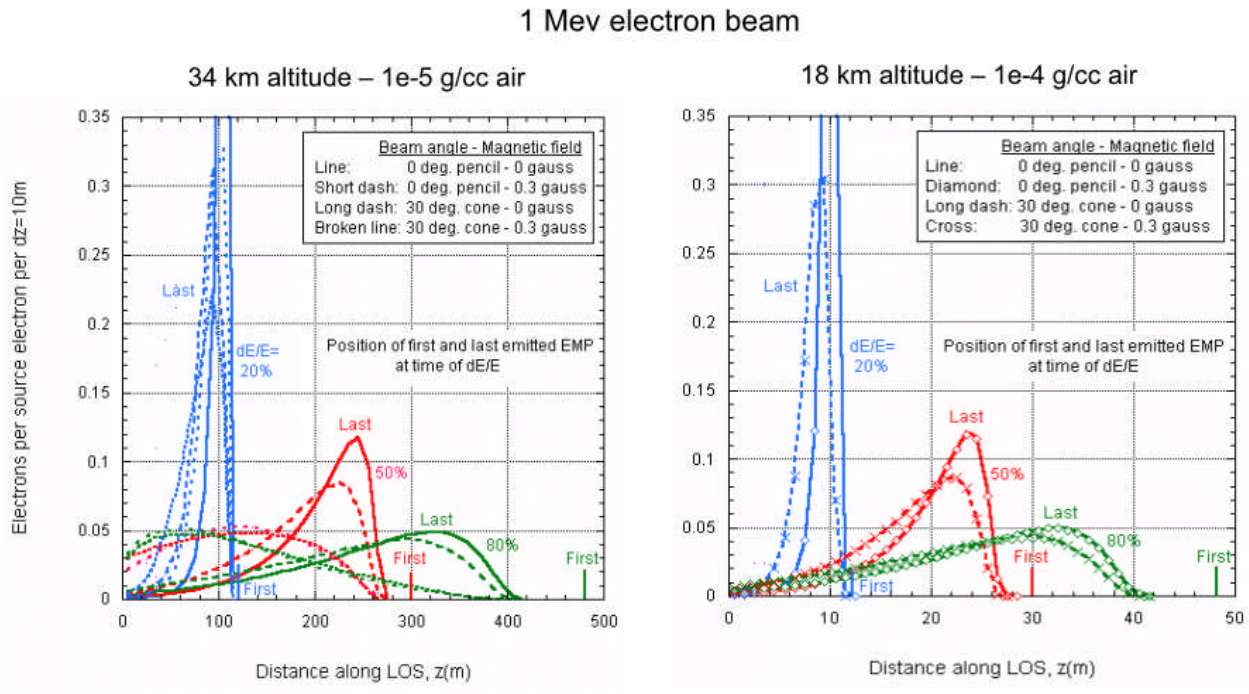

Fig. 4. Bending by the earth's magnetic field also spreads the electrons along the LOS. This is significant only for high altitudes. However, EMP generated at high altitudes can propagate to the ground observer only for low yields. For high yields it is absorbed by the air conductivity.

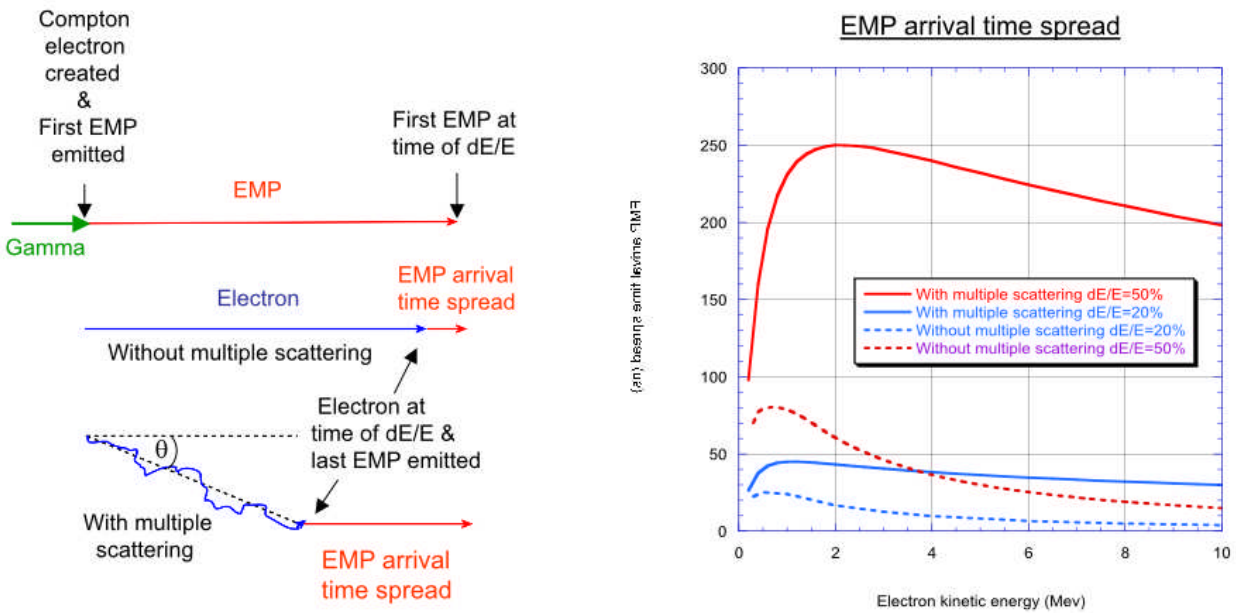

Fig. 5. EMP arrival time spread at the observer with and without adjusting the position of the radiating electron for multiple scattering, based on spread sheet calculations using a root-mean-square scattering angle and tabulated stopping powers. The air density is 1.2e-5 g/cc corresponding to an altitude of ~33 km.

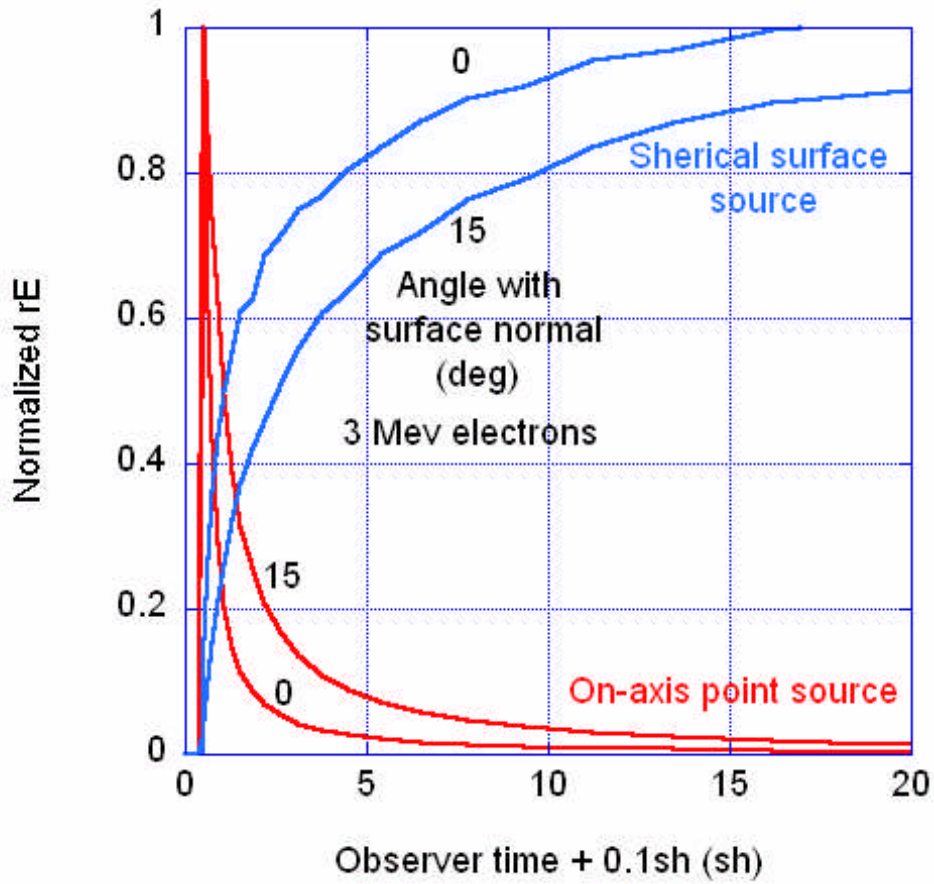

Fig. 6. These MACSYNC calculations show how the rise time of the composite EMP at the observer arises from the superposition of EMP emitted by point sources distributed over a spherical surface. The source is an electron pencil beam directed either along the LOS at the observer or uniformly distributed in angle between the LOS and an angle of 15 degrees with the LOS. The air density is 1.2e-5 g/cc corresponding to an altitude of 33 km. There is no EMP attenuation between the source and the observer.

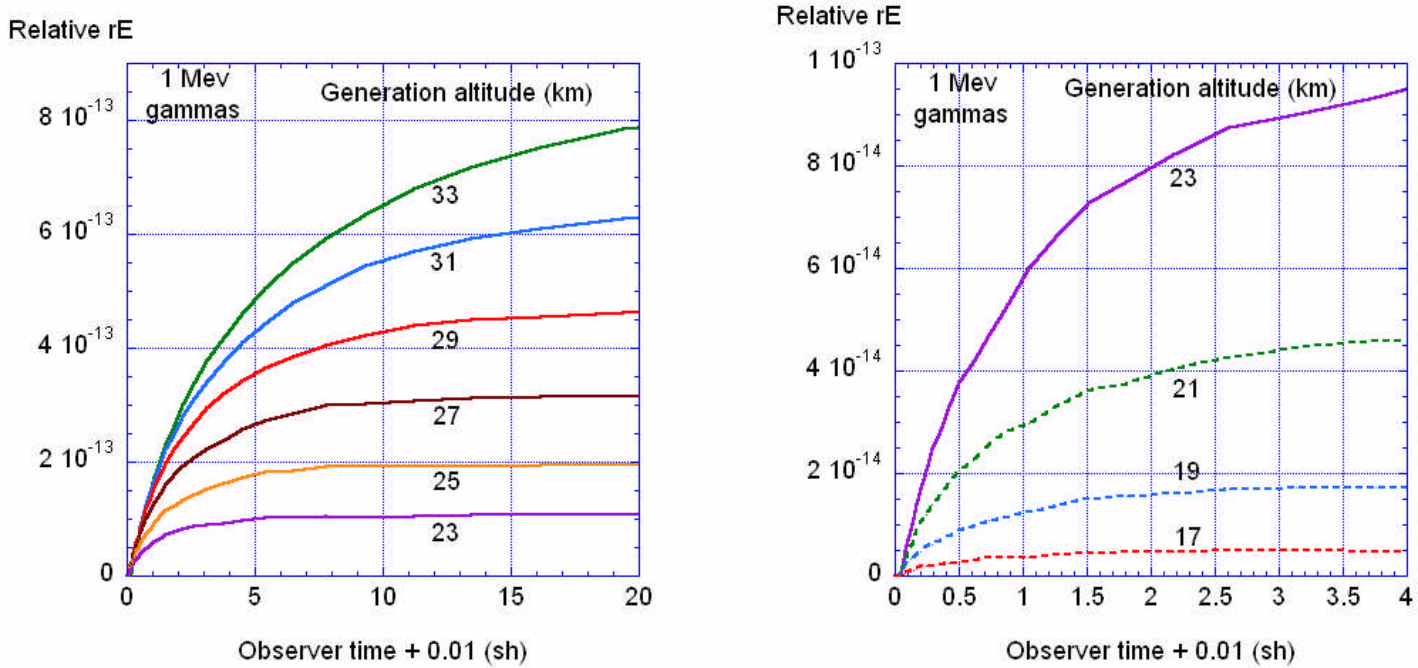

Fig. 7. MACSYNC calculations of EMP generated in 2 km high altitude bands in an exponential atmosphere by an isotropic 1 Mev gamma point source with a 0.01 sh step pulse width at 100 km altitude. There is no EMP attenuation. Ground observer directly below burst point.

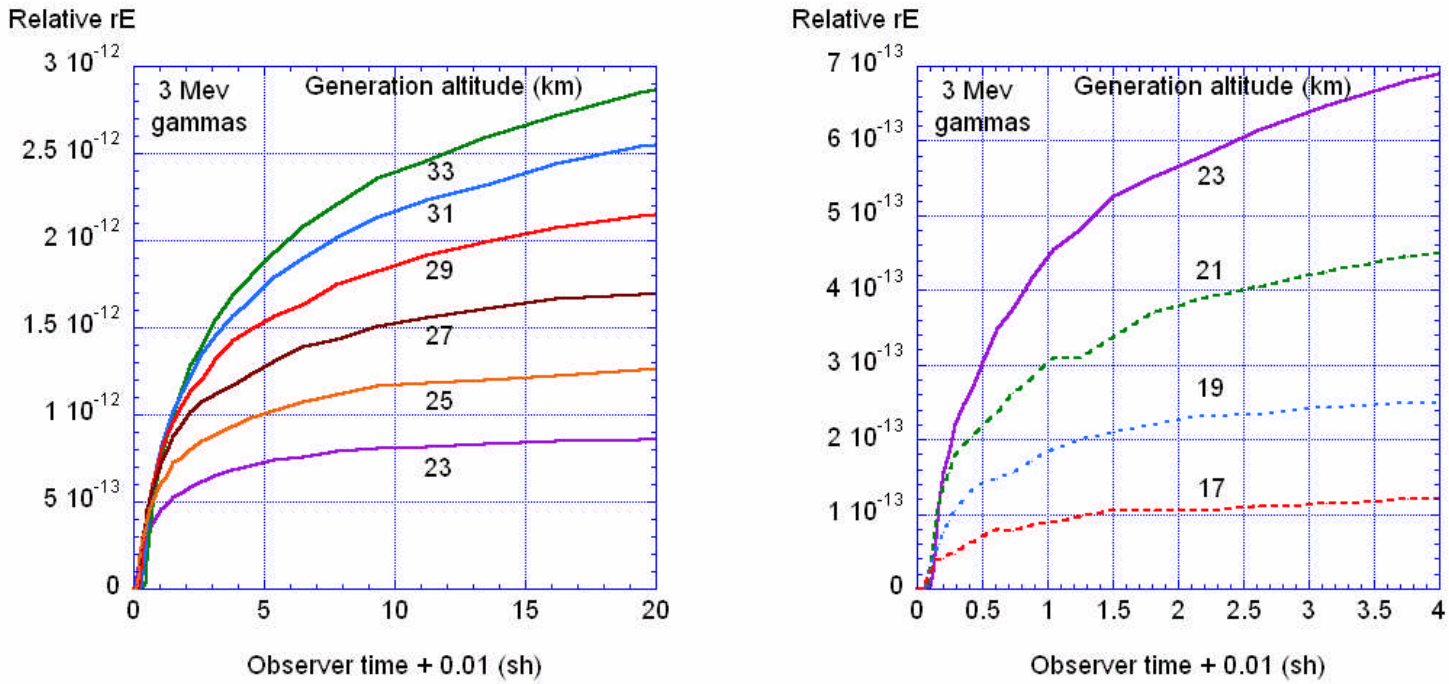

Fig. 8. Same as Fig. 7, except that the gamma energy is 3 Mev.

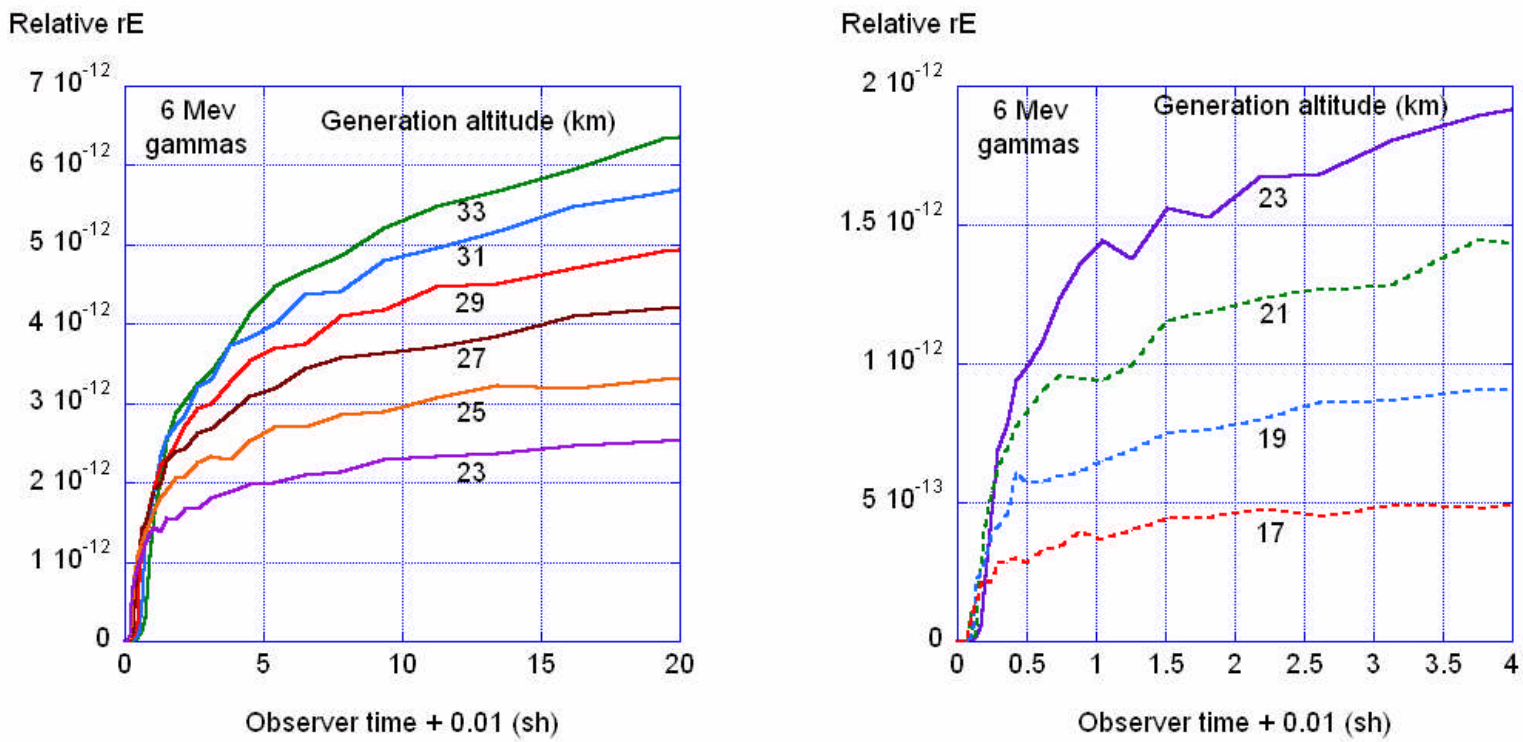

Fig. 9. Same as Fig. 7, except the gamma energy is 6 Mev.

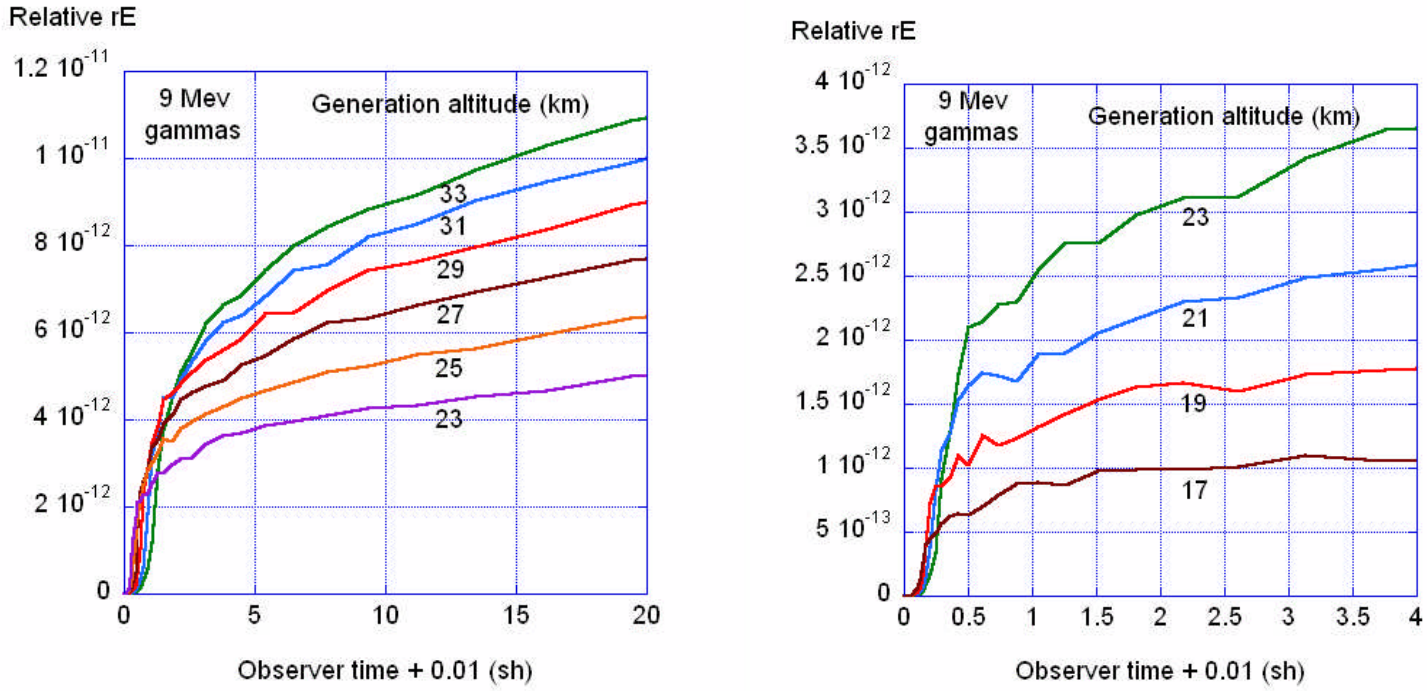

Fig. 10. Same as Fig. 7, except the gamma energy is 9 Mev.

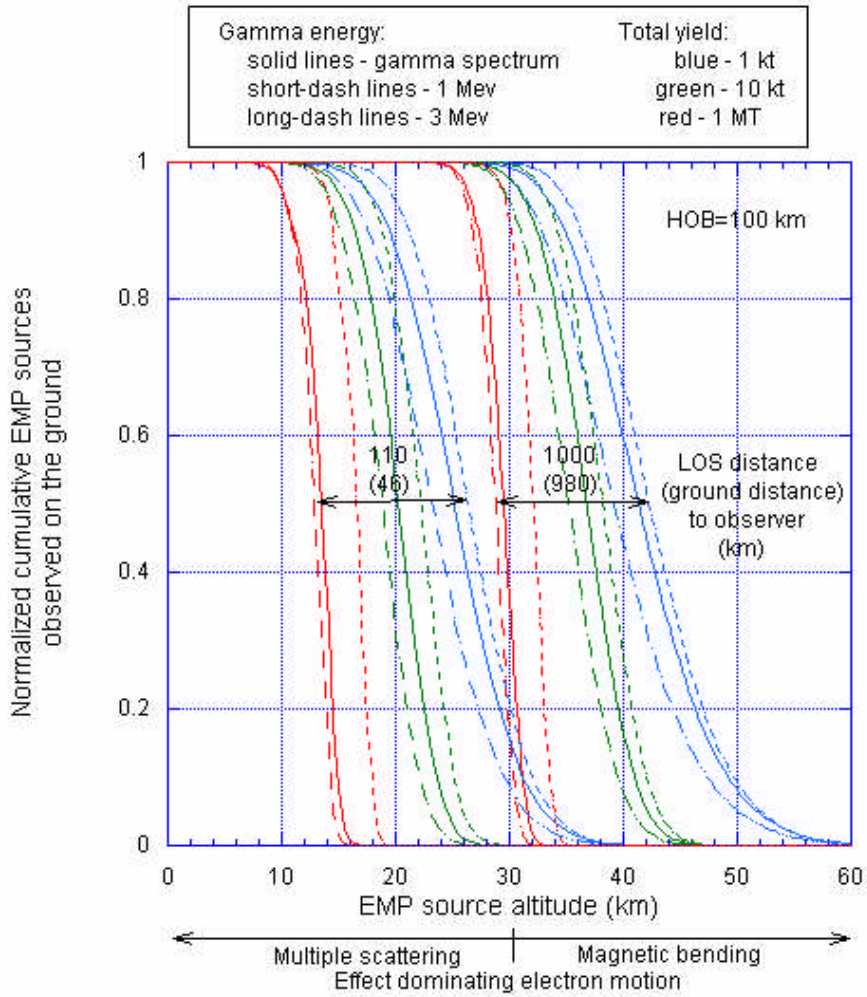

Fig. 11. These EMATT calculations show that increased yields prevent EMP, generated at higher altitudes, from reaching the ground observer. This is due to the increased air conductivity absorbing the EMP from higher altitudes.

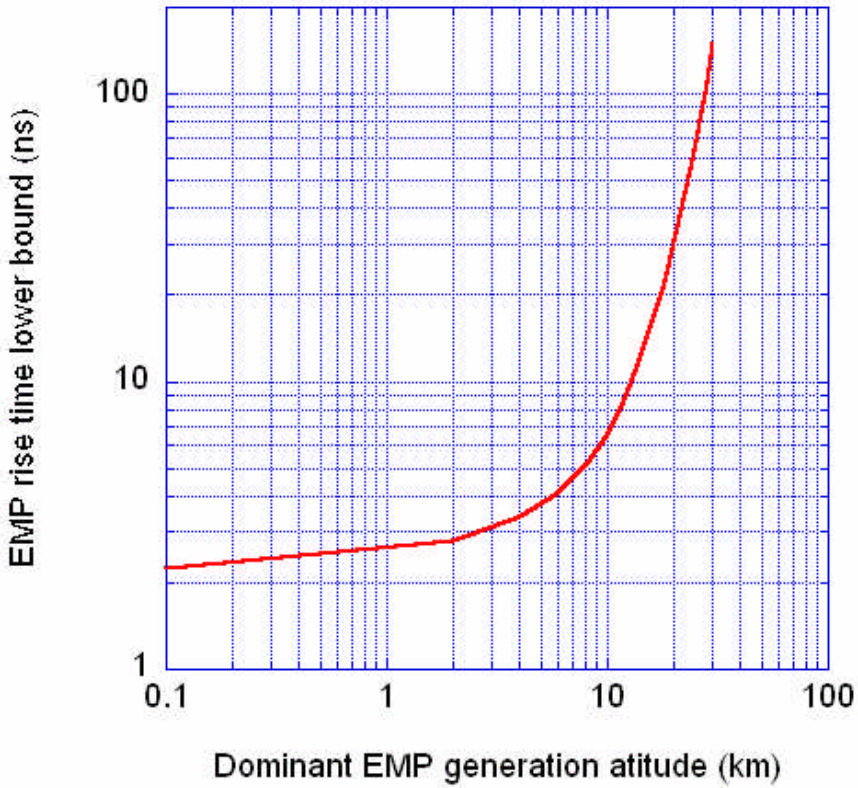

Fig. 12. EMP lower rise time bound estimate based on inspection of MACSYNC calculations shown in Figs. 7-10.

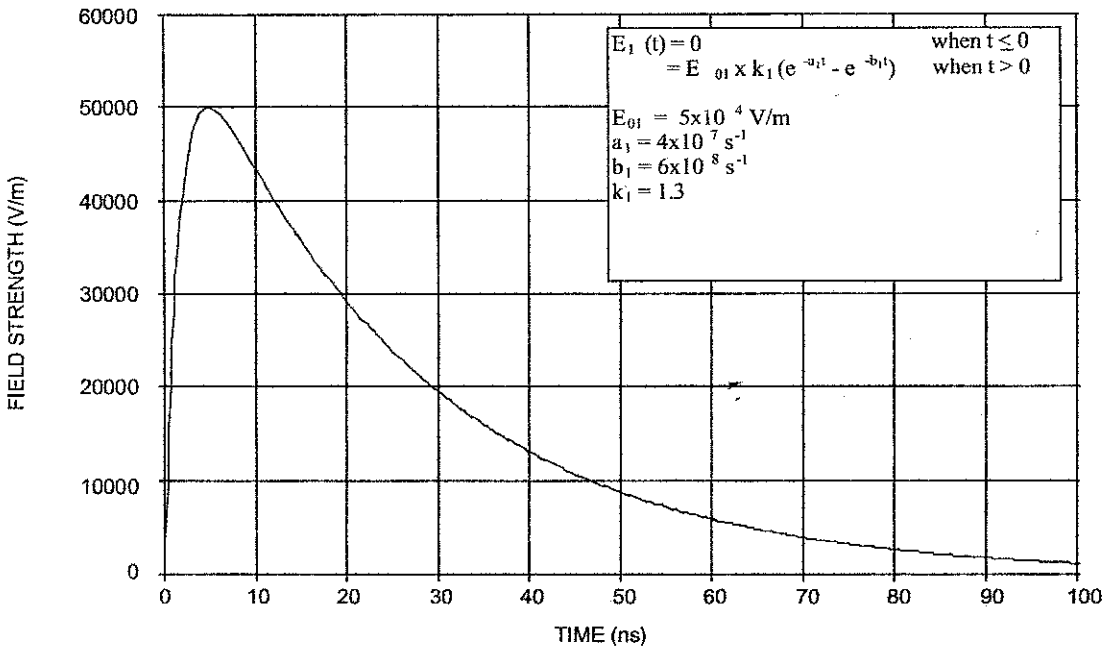

Fig. 13. EMP hardening standard MIL-STD-464 specifies this default free-field EMP environment, which is derived from calculations with legacy 1D-spherical geomagnetic EMP codes. This short rise time of nanoseconds is an unphysical artifact caused by physics simplifications in the legacy codes.

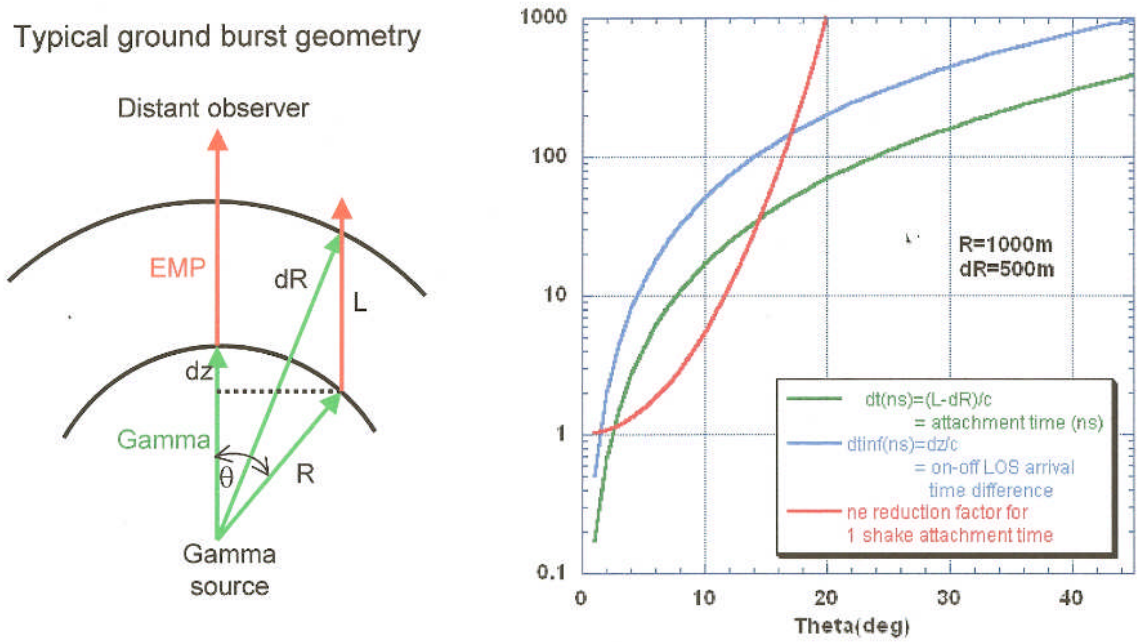

Fig. 14. 3D geometry produces EMP arrival delays at a given radius between on- and off-LOS propagation paths. Off-LOS EMP arrives later when attachment has reduced the conduction electron column density and associated attenuation along the path to the observer. The yield used in the graph is 1 kT.

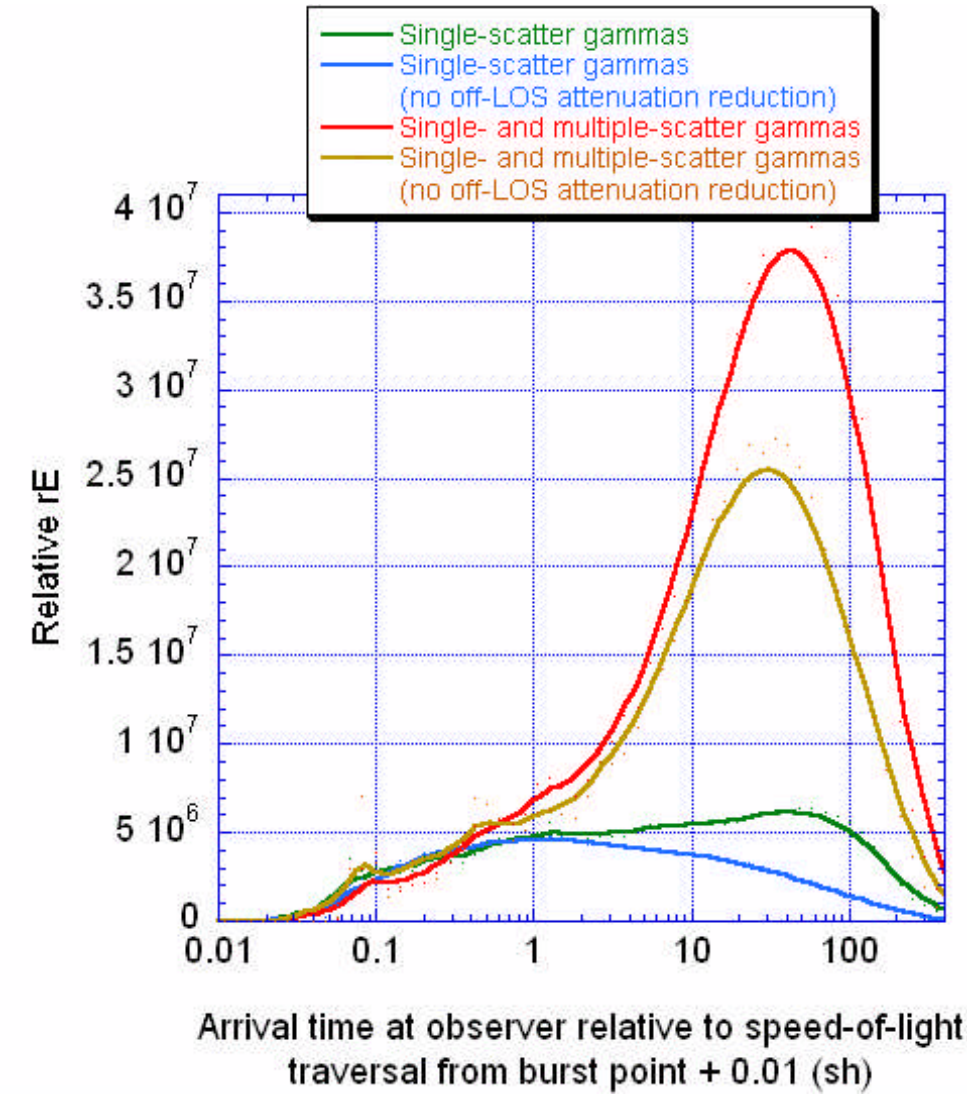

FIG. 15. MACSYNC calculations used a total yield of 1 kT detonated at sea level, 0.03% gamma fraction, and a 0.01 sh step output pulse of 3 Mev gammas. The calculations either stopped gamma transport after the first Compton scatter or they allowed mutiple gamma transport. For either case, the off-LOS EMP attenuation reduction was either turned on or off.

Distribution